Overexpression of γ-tocopherol methyl transferase gene in transgenic *Brassica juncea* plants alleviates abiotic stress: Physiological and chlorophyll a fluorescence measurements

Mohd. Aslam Yusuf [a,1], Deepak Kumar [a], Ravi Rajwanshi [a], Reto Jörg Strasser [b], Merope Tsimilli-Michael [b,2], Govindjee [c], Neera Bhalla Sarin [a,*]

[a] *School of Life Sciences, Jawaharlal Nehru University, New Delhi-110067, India*
[b] *Bioenergetics Laboratory, University of Geneva, CH-1254 Jussy/Geneva, Switzerland*
[c] *Department of Plant Biology, University of Illinois at Urbana-Champaign, Urbana, IL-61801, USA*

ABSTRACT

Tocopherols (vitamin E) are lipid soluble antioxidants synthesized by plants and some cyanobacteria. We have earlier reported that overexpression of the γ-tocopherol methyl transferase (γ-TMT) gene from *Arabidopsis thaliana* in transgenic *Brassica juncea* plants resulted in an over six-fold increase in the level of α-tocopherol, the most active form of all the tocopherols. Tocopherol levels have been shown to increase in response to a variety of abiotic stresses. In the present study on *Brassica juncea*, we found that salt, heavy metal and osmotic stress induced an increase in the total tocopherol levels. Measurements of seed germination, shoot growth and leaf disc senescence showed that transgenic *Brassica juncea* plants overexpressing the γ-TMT gene had enhanced tolerance to the induced stresses. Analysis of the chlorophyll *a* fluorescence rise kinetics, from the initial "O" level to the "P" (the peak) level, showed that there were differential effects of the applied stresses on different sites of the photosynthetic machinery; further, these effects were alleviated in the transgenic (line 16.1) *Brassica juncea* plants. We show that α-tocopherol plays an important role in the alleviation of stress induced by salt, heavy metal and osmoticum in *Brassica juncea*.

© 2010 Elsevier B.V. All rights reserved.

1. Introduction

Vitamin E includes tocopherols, one of the most powerful antioxidants, and tocotrienols [1]. The most important function of tocopherols in biological membranes is that they act as recyclable chain reaction terminators of polyunsaturated fatty acid (PUFA) free radicals generated by lipid oxidation [1,2]. Tocopherols α, β, γ, and δ have different in vivo antioxidant activities against lipid oxidation with one molecule of each of these tocopherols protecting up to 220, 120, 100, and 30 molecules of PUFA, respectively [3]. Tocopherols have been suggested to play a major role in the maintenance and protection of the photosynthetic machinery. Although plants and cyanobacteria are the sole source of tocopherols, research on the function of tocopherols in these organisms has begun only recently. Abiotic stress (e.g., high intensity light, salinity, drought or low temperature) has been shown to lead to increased tocopherol content in plastid membranes, which are also enriched in PUFAs [4,5]. There is clearly a correlation between the degree of stress and the tocopherol concentration [6]. Gajewska and Sklodowska [7] and Collin et al. [8] have suggested that increased tocopherol content confers enhanced tolerance to plants against drought and heavy metal (Ni, Cu, Cd) stress. Singlet molecular oxygen ($^1O_2$), produced in the thylakoids when plants are exposed to high light, can oxidize membrane lipids, proteins, amino acids, nucleic acids, nucleotides, carbohydrates and thiols and, thus, damage plants [9,10]. Tocopherols are able to physically quench or chemically scavenge $^1O_2$ [11,12]. Kruk and Strzalka [13] showed that α-tocopherol quinone, present in chloroplasts, oxidizes cytochrome (cyt) b_{559}, and plays a role in cyclic electron flow around Photosystem (PS) II when the photosynthetic electron transport chain is over-reduced. Fryer [2] suggested that α-tocopherol could also reduce the permeability of thylakoid membrane to ions and, thereby, affect the maintenance of ΔpH, the light generated transmembrane proton gradient. The ΔpH is responsible not only for ATP synthesis, but also for the conversion of violaxanthin to zeaxanthin in the xanthophyll cycle, which is further involved in

the harmless dissipation of excess excitation energy, as heat, in the thylakoids (see e.g. [14,15] for review). The methylation of γ-tocopherol to α-tocopherol, which is the rate limiting final step of α-tocopherol biosynthesis, is catalyzed by the γ-tocopherol methyl transferase (γ-TMT). In an effort to increase the α-tocopherol in *Brassica juncea* seed oil, transgenic *B. juncea* plants constitutively overexpressing the γ-TMT gene were generated by Yusuf and Sarin [16]. In the present work, we have used these transgenic (TR) plants for investigation of the role of α-tocopherol in the protection of the photosynthetic machinery against abiotic stress. We have focused our study mainly on the TR line 16.1, in which overexpression of the γ-TMT gene was highest [16]. We applied salt (NaCl), heavy metal (CdCl$_2$) and osmotic (mannitol) stress on the TR and wild type (WT) plants and made comparative studies of the regulation of tocopherol levels and the tolerance to abiotic stress.

We have evaluated the photosynthetic activity of WT and TR (line 16.1) *B. juncea* plants from the analysis of chlorophyll (Chl) *a* fluorescence rise kinetics [17,18], from the initial "O" level to the "P" (the peak) level, called OJIP kinetics [19]. This analysis [17,18], referred to as the "JIP-test" allows us to obtain information on the structural and functional parameters that quantify the performance/ activity of the photosynthetic machinery (for explanation, see the Materials and methods section, where the formulae and glossary of terms used by the JIP-test are presented). It is well known that Chl *a* fluorescence measurements are non-invasive, efficient, rapid and sensitive; further, the JIP-test has been widely used for evaluation of the impact of different types of stress, such as, high light, high or low temperature, ozone, drought, salinity and heavy metals. It has also been used to study stress alleviation (see Strasser et al. [17] and references therein; also see [18,20,21]). In this paper, the JIP-test has been used to obtain information on the effects of the applied stresses on different sites of the photosynthetic machinery. It has revealed that in the TR (line 16.1) plants of *B. juncea*, the stress effects were alleviated, while the photosynthetic performance on the basis of light absorption was found to be even higher than in unstressed WT plants.

2. Materials and methods

2.1. Plant material

Transgenic *B. juncea* plants overexpressing the γ-TMT gene were generated as described by Yusuf and Sarin [16]. Both the WT and the TR plants were used in our studies.

2.2. Determination of tocopherols

Seedlings of WT and TR (line 16.1) *B. juncea* were grown for 5 days hydroponically on a nylon mesh, used as a support on which the seeds were kept. This was placed over a box filled with Hoagland solution; as the seeds germinated, the roots went beneath, through the mesh, into the solution. The solution was aerated using an aquarium air pump. On day 5, the Hoagland solution, which was changed every day, was removed and the boxes were filled with solutions containing different concentrations of NaCl, CdCl$_2$ and mannitol in water, for inducing salt, heavy metal and osmotic stress, respectively. The cotyledonary leaves, collected after 72 h, were frozen in liquid nitrogen and tocopherol concentration was measured in these samples using High Performance Liquid Chromatography (HPLC), as described earlier [16]. The experiment was repeated three times, using 1 g of cotyledonary leaves for each measurement.

2.3. Seed germination

Seeds from the WT and TR (line 16.1) *B. juncea* plants were surface sterilized and placed in MS (Murashige and Skoog, [22]) basal medium, with additional 200 mM NaCl, 20 mM CdCl$_2$ or 200 mM mannitol, for germination. We report percent germination based on three experiments (50–60 seeds taken for each replicate).

2.4. Shoot growth

Seeds from WT and three independent TR lines, 16.1, 14.1 and 25.1, of *B. juncea* plants were germinated on MS basal medium. On day 5, the shoots were cut from below the cotyledonary leaves and placed on the same medium supplemented with 400 mM NaCl, 40 mM CdCl$_2$, or 200 mM mannitol. Growth was visually followed up to day 15.

2.5. Chlorophyll content

Discs of equal diameter from fully grown mature leaves of untreated WT and TR plants were floated on water and on solutions with different concentrations of NaCl, CdCl$_2$, or mannitol. The chlorophyll content in leaf discs (weighing 200 mg) was estimated, in 3 different experiments, after 7 days of treatment, using the method of Arnon [23].

2.6. Measurement of the fast chlorophyll a fluorescence transients

For chlorophyll fluorescence measurements, WT and TR (line 16.1) plants were grown in a glasshouse under $28/15 \pm 2$ °C (day/night) regime. Thirty day old plants were subjected to stress treatments, by watering them with solutions of salt (NaCl; 200 mM), heavy metal (CdCl$_2$; 20 mM) or mannitol (200 mM) every fortnight; plants not subjected to any of the treatments served as the experimental control. Forty-five days after the start of the treatments, Chl *a* fluorescence measurements were made on intact young leaves still attached to the plants and adapted to dark for 1 h. Three plants from each plant type and treatment were used and six measurements per plant were taken (18 replicates).

The OJIP fluorescence transients (10 µs to 1 s) were measured with a Handy-PEA fluorimeter (Plant Efficiency Analyser, Hansatech Instruments Ltd., King's Lynn Norfolk, PE 30 4NE, UK). We note that O is the initial fluorescence level, J (2 ms) and I (30 ms) are intermediate levels, and P (500 ms–1 s) is the peak level [19]. The transients in leaves were induced by red light (peak at 650 nm) of 3000 µmol photons m^{-2} s^{-1} provided by an array of 3 light-emitting diodes, focused on a spot of 5 mm diameter, and recorded for 1 s with 12 bit resolution. The data acquisition was at every 10 µs (from 10 µs to 0.3 ms), every 0.1 ms (from 0.3 to 3 ms), every 1 ms (from 3 to 30 ms), every 10 ms (from 30 to 300 ms) and every 100 ms (from 300 ms to 1 s). The OJIP transients were analyzed using the JIP-test (see below).

2.7. Analysis of chlorophyll fluorescence data

2.7.1. The basics

The investigation of Chl *a* fluorescence induction (Kautsky curve) has provided a wealth of information about the structure and function of the photosynthetic machinery; hence the Chl *a* fluorescence has been labeled as a "signature of photosynthesis" [24]. The JIP-test is a multiparametric analysis of the fast fluorescence rise OJIP, developed by Strasser and co-workers (for a detailed explanation of the JIP-test, see [17] and references therein; see also [18,20]). In the dark, the primary quinone electron acceptor of PS II (Q$_A$) is assumed to be oxidized (when all reactions centers (RCs) are open) and the fluorescence intensity at the onset of illumination F_0 (at the origin-O) is minimal. The fast fluorescence rise induced by actinic light reflects the closure of the RCs (reduction of Q$_A$). Under strong actinic light (e.g. 3000 µmol photons m^{-2} s^{-1}), the fluorescence intensity F_P (at the peak-P) is equal to the maximum fluorescence, F_M, when all Q$_A$ is reduced (all RCs are closed). The sequential events reflected in the

fluorescence rise proceed with different rates and, concomitantly, the rise is polyphasic [19].

The OJ phase (induced by strong actinic light) is suggested to reflect a single turnover photochemical event, since (i) the J-step appears at the same time as F_M in samples when reoxidation of Q_A^- is blocked by an inhibitor, such as 3-(3,4-dichlorophenyl)-1,1-dimethylurea (DCMU) and (ii) OJ phases of samples, with and without DCMU, are identical when these curves are normalized between O and J levels. The JI phase is considered to mainly reflect the reduction of the intersystem electron carriers, i.e., the secondary quinone electron acceptor-Q_B, plastoqui-none-PQ, cytochrome-Cyt and plastocyanin-PC, while the IP phase reflects the reduction of PS I electron acceptors i.e., ferredoxin-Fd, other intermediates and NADP.

The JIP-test, which incorporates the above interpretations, was applied in this study for the analysis and comparison of the OJIP transients in different samples. The JIP-test involves two different ways of data processing, as described below.

2.7.2. Utilization of the whole fluorescence transient: normalizations and subtractions

To compare the samples for the events, reflected in the OJ, OI and IP phases (see Section 2.7.1), the transients were normalized as relative variable fluorescence (general symbol W): $W_{OJ} = (F_t - F_0)/(F_J - F_0)$, $W_{OI} = (F_t - F_0)/(F_I - F_0)$ and $W_{IP} = (F_t - F_I)/(F_P - F_I)$. In addition, we also calculated difference kinetics, $\Delta W = W - W_{ref}$ ("ref" is for untreated WT). The difference kinetics reveal bands that are usually hidden between the steps O, J, I and P of the raw or normalized transients [17,18,20]. The difference kinetics ΔW_{OJ} reveals the K-band (at about 300 µs) which, when positive, is considered to reflect an inactivation of the oxygen evolving complex (especially of the Mn-complex) and/or an increase of the functional PS II antenna size. After heat treatment, or at high temperature, when inactivation of the oxygen evolving complex is induced (see e.g. [17]), the K-step appears even in direct fluorescence transients (then called OKJIP).

The shape of the OJ phase carries information on the energetic connectivity (grouping) between the PS II photosynthetic units: it is exponential when there is no connectivity (separate units) and sigmoidal when there is connectivity [17,25]. A sigmoidal and an exponential curve (induced by the same actinic light as that used in the present work) cross at 300 µs [33]. Therefore, the normalization between the "O" (50 µs) and the "K" (300 µs) steps, which transforms the OK phase to the kinetics $W_{OK} = (F_t - F_0)/(F_K - F_0)$, allows us to compare the samples for energetic connectivity of PS II. The difference kinetics $W_{OK} - (W_{OK})_{ref}$ reveals another band, the L-band (at about 150 µs), which is positive (or negative) when the energetic connec-tivity of the sample is lower (or higher) than that of the WT plant. A higher connectivity results in a better utilization of the excitation energy and a higher stability of the system [17].

2.7.3. The JIP-test equations — utilization of selected fluorescence signals

The JIP-test equations are based on the Theory of Energy Fluxes in Biomembranes [25]. Therefore, the definitions and equations of the JIP-test are shown using a scheme (Fig. 1; modified after [18]), which is the well-known Z-scheme of photosynthesis, expressed here by sequential energy fluxes (wide arrows). Formulae and glossary of terms used by the JIP-test are presented in Table 1.

The energy cascade starts from absorption (ABS) of light by PS II antenna pigments and ends at the reduction of the end electron acceptors at the PS I electron acceptor side (RE) driven by PS I. Intermediate energy fluxes are the trapping flux (TP), defined as the energy flux leading to the reduction of the electron acceptors of PS II, pheophytin-Pheo and Q_A, and the electron transport flux (ET) that refers (by our definition, see Table 1) to the electron transport further than Q_A^- (see also the column "definition of events and corresponding energy fluxes" in Fig. 1).

The energy influx, at each of the steps, is either used for electron transfer (grey arrows) and thus conserved, or is dissipated (white arrows; note that TP-ET is the energy flux leading to the accumulation of Q_A^-). The efficiency of energy conservation at each step is also indicated (next to the line arrows between the sequential steps), where φ refers to quantum yields (efficiencies on the basis of light absorption; i.e., fluxes per ABS), ψ to efficiencies per TP and δ to efficiency per ET. The fraction of energy influx that is dissipated and, therefore, does not lead to energy conservation via electron transfer
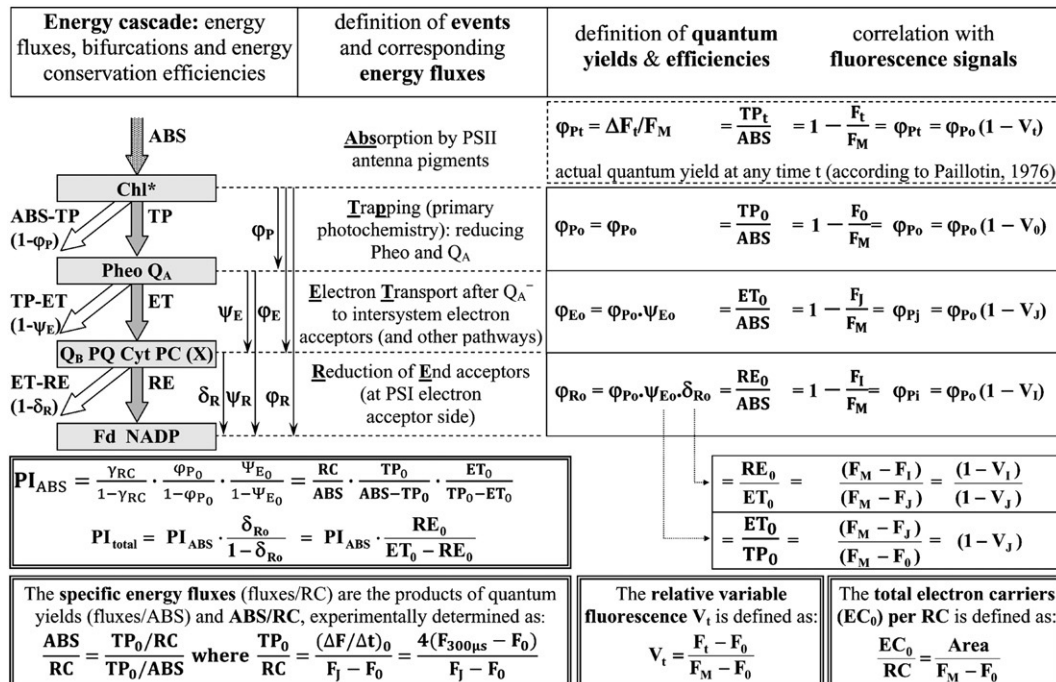

Energy cascade: energy fluxes, bifurcations and energy conservation efficiencies	definition of events and corresponding energy fluxes	definition of quantum yields & efficiencies		correlation with fluorescence signals
ABS	Absorption by PSII antenna pigments	$\varphi_{Pt} = \Delta F_t/F_M$	$= \dfrac{TP_t}{ABS} = 1 - \dfrac{F_t}{F_M} = \varphi_{Pt} = \varphi_{Po}(1 - V_t)$ actual quantum yield at any time t (according to Paillotin, 1976)	
Chl*				
ABS-TP (1-φ_P) / TP $\quad \varphi_P$	Trapping (primary photochemistry): reducing Pheo and Q_A	$\varphi_{Po} = \varphi_{Po}$	$= \dfrac{TP_0}{ABS} = 1 - \dfrac{F_0}{F_M} = \varphi_{Po} = \varphi_{Po}(1 - V_0)$	
Pheo Q_A				
TP-ET (1-ψ_E) / ET $\quad \psi_E \; \varphi_E$	Electron Transport after Q_A^- to intersystem electron acceptors (and other pathways)	$\varphi_{Eo} = \varphi_{Po} \cdot \psi_{Eo}$	$= \dfrac{ET_0}{ABS} = 1 - \dfrac{F_J}{F_M} = \varphi_{Pj} = \varphi_{Po}(1 - V_J)$	
Q_B PQ Cyt PC (X)				
ET-RE (1-δ_R) / RE $\quad \delta_R \; \psi_R \; \varphi_R$	Reduction of End acceptors (at PSI electron acceptor side)	$\varphi_{Ro} = \varphi_{Po} \cdot \psi_{Eo} \cdot \delta_{Ro} = \dfrac{RE_0}{ABS} = 1 - \dfrac{F_I}{F_M} = \varphi_{Pi} = \varphi_{Po}(1 - V_I)$		
Fd NADP				

$$PI_{ABS} = \frac{\gamma_{RC}}{1-\gamma_{RC}} \cdot \frac{\varphi_{Po}}{1-\varphi_{Po}} \cdot \frac{\Psi_{Eo}}{1-\Psi_{Eo}} = \frac{RC}{ABS} \cdot \frac{TP_0}{ABS-TP_0} \cdot \frac{ET_0}{TP_0-ET_0}$$

$$PI_{total} = PI_{ABS} \cdot \frac{\delta_{Ro}}{1-\delta_{Ro}} = PI_{ABS} \cdot \frac{RE_0}{ET_0-RE_0}$$

$$= \frac{RE_0}{ET_0} = \frac{(F_M - F_I)}{(F_M - F_J)} = \frac{(1 - V_I)}{(1 - V_J)}$$

$$= \frac{ET_0}{TP_0} = \frac{(F_M - F_J)}{(F_M - F_0)} = (1 - V_J)$$

The **specific energy fluxes** (fluxes/RC) are the products of quantum yields (fluxes/ABS) and **ABS/RC**, experimentally determined as: $$\frac{ABS}{RC} = \frac{TP_0/RC}{TP_0/ABS} \text{ where } \frac{TP_0}{RC} = \frac{(\Delta F/\Delta t)_0}{F_J - F_0} = \frac{4(F_{300µs} - F_0)}{F_J - F_0}$$	The **relative variable fluorescence** V_t is defined as: $$V_t = \frac{F_t - F_0}{F_M - F_0}$$	The **total electron carriers** (EC_0) per RC is defined as: $$\frac{EC_0}{RC} = \frac{Area}{F_M - F_0}$$

Fig. 1. A schematic presentation of the JIP-test (modified after Tsimilli-Michael and Strasser [18]).

Table 1

Formulae and glossary of terms used by the JIP-test for the analysis of Chl *a* fluorescence transient OJIP emitted by dark-adapted photosynthetic samples (modified after Strasser et al. [17]).

Data extracted from the recorded fluorescence transient OJIP	
F_t	Fluorescence at time t after onset of actinic illumination
$F_{50\ \mu s}$ or $F_{20\ \mu s}$	Minimal reliable recorded fluorescence, at 50 μs with the PEA- or 20 μs with the Handy-PEA-fluorimeter
$F_{300\ \mu s}$	Fluorescence intensity at 300 μs
$F_J \equiv F_{2\ ms}$	Fluorescence intensity at the J-step (2 ms) of OJIP
$F_I \equiv F_{30\ ms}$	Fluorescence intensity at the I-step (30 ms) of OJIP
F_P	Maximal recorded fluorescence intensity, at the peak P of OJIP
t_{FM}	Time (in ms) to reach the maximal fluorescence intensity F_M
Area	Total complementary area between the fluorescence induction curve and $F = F_M$
Fluorescence parameters derived from the extracted data	
$F_0 \cong F_{50\ \mu s}$ or $\cong F_{20\ \mu s}$	Minimal fluorescence (all PSII RCs are assumed to be open)
$F_M\ (=F_P)$	Maximal fluorescence, when all PSII RCs are closed (equal to F_P when the actinic light intensity is above 500 μmol photons $m^{-2}\ s^{-1}$ and provided that all RCs are active as Q_A reducing)
$F_v \equiv F_t - F_0$	Variable fluorescence at time t
$F_V \equiv F_M - F_0$	Maximal variable fluorescence
$V_t \equiv F_v/F_V \equiv (F_t - F_0)/(F_M - F_0)$	Relative variable fluorescence at time t
$M_0 \equiv [(\Delta F/\Delta t)_0]/(F_M - F_{50\ \mu s})$ $\equiv 4(F_{300\ \mu s} - F_{50\ \mu s})/(F_M - F_{50\ \mu s})$	Approximated initial slope (in ms^{-1}) of the fluorescence transient normalized on the maximal variable fluorescence F_V
Specific energy fluxes (per Q_A-reducing PSII reaction center — RC)	
$ABS/RC = M_0\ (1/V_J)(1/\varphi_{Po})$	Absorption flux (of antenna Chls) per RC
$TP_0/RC = M_0\ (1/V_J)$	Trapping flux (leading to Q_A reduction) per RC
$ET_0/RC = M_0\ (1/V_J)\psi_{Eo}$	Electron transport flux (further than Q_A^-) per RC
$RE_0/RC = M_0\ (1/V_J)\psi_{Eo}\ \delta_{Ro}$	Electron flux reducing end electron acceptors at the PSI acceptor side, per RC
Quantum yields and efficiencies	
$\varphi_{Pt} \equiv TP_t/ABS = [1 - (F_t/F_M)] = \Delta F_t/F_M$	Quantum yield for primary photochemistry at any time t, according to the general equation of Paillotin [26]
$\varphi_{Po} \equiv TP_0/ABS = [1 - (F_0/F_M)]$	Maximum quantum yield for primary photochemistry
$\psi_{Eo} \equiv ET_0/TP_0 = (1 - V_J)$	Efficiency/probability for electron transport (ET), i.e. efficiency/probability that an electron moves further than Q_A^-
$\varphi_{Eo} \equiv ET_0/ABS = [1 - (F_0/F_M)]\psi_{Eo}$	Quantum yield for electron transport (ET)
$\delta_{Ro} \equiv RE_0/ET_0 = (1 - V_I)/(1 - V_J)$	Efficiency/probability with which an electron from the intersystem electron carriers moves to reduce end electron acceptors at the PSI acceptor side (RE)
$\varphi_{Ro} \equiv RE_0/ABS = [1 - (F_0/F_M)]\psi_{Eo}\ \delta_{Ro}$	Quantum yield for reduction of end electron acceptors at the PSI acceptor side (RE)
$\gamma_{RC} = Chl_{RC}/Chl_{total} = RC/(ABS + RC)$	Probability that a PSII Chl molecule functions as RC
$RC/ABS = \gamma_{RC}/(1 - \gamma_{RC}) = \varphi_{Po}\ (V_J/M_0)$	Q_A-reducing RCs per PSII antenna Chl (reciprocal of ABS/RC)
Performance indexes (products of terms expressing partial potentials at steps of energy bifurcations)	
$PI_{ABS} \equiv \frac{\gamma_{RC}}{1 - \gamma_{RC}} \cdot \frac{\varphi_{Po}}{1 - \varphi_{Po}} \cdot \frac{\psi_o}{1 - \psi_o}$	Performance index (potential) for energy conservation from exciton to the reduction of intersystem electron acceptors
$PI_{total} \equiv PI_{ABS} \cdot \frac{\delta_{Ro}}{1 - \delta_{Ro}}$	Performance index (potential) for energy conservation from exciton to the reduction of PSI end acceptors

Subscript "0" indicates that the parameter refers to the onset of illumination.

(white arrow), is indicated in brackets under the corresponding outflux (see Fig. 1).

The scheme also includes the equations by which the quantum yields and the other efficiencies at the onset of illumination (all RCs open; subscript "0") are defined and further linked with fluorescence signals selected from the OJIP fluorescence transients, F_0, F_J, F_I and F_M ($= F_P$). The equations (in Fig. 1) by which the quantum yields are linked with fluorescence signals are based on the general equation given by Paillotin [26]. According to this equation, the quantum yield at any time t, where the fluorescence intensity is F_t (between F_0 and F_M), is calculated by $\varphi_{Pt} = 1 - F_t/F_M = \Delta F_t/F_M$ (also known as the "Genty equation"; see [27]). The Paillotin equation further links (as shown) the quantum yield at any time t with the maximum quantum yield and the complement of the relative variable fluorescence, V_t, at that time, as $\varphi_{Pt} = \varphi_{Po}\ (1 - V_t)$. The formula by which V_t is defined on the basis of fluorescence signals, $V_t = (F_t - F_0)/(F_M - F_0)$, is given at the bottom of the figure, along with the formulae defining the following parameters of the JIP-test [17] used in the present work:

- *The total electron carriers per reaction centre (EC_0/RC)*: This is equal to the complementary area (Area) above the fluorescence transient, i.e., the area between the curve, the horizontal line $F = F_M$ and the vertical lines at $t = 50$ μs and at $t = t_{FM}$ (the time at which F_M is reached), divided by the maximum variable fluorescence, $F_V = F_M - F_0$.
- *The specific energy fluxes (energy fluxes per RC; arbitrary units)*: They are derived by multiplying the corresponding quantum yields (energy fluxes per ABS) by the specific absorption flux ratio, ABS/RC. The calculation of the latter is based, as also shown in

Fig. 1, on the calculation (in arbitrary units) of the specific flux for trapping, $TP_0/RC = [(\Delta F/\Delta t)_0]/(F_J - F_0) = 4(F_{300\ \mu s} - F_0)/(F_J - F_0)$. The basis for this formula is that the OJ phase reflects single turnover photochemical events (see above); therefore, TP_0/RC is proportional to the initial slope (taken between 50 and 300 μs and expressed in ms^{-1}) of the normalized transient $(F_t - F_0)/(F_J - F_0)$.

- *The performance indices PI_{ABS} and PI_{total}*: These indices are products of terms expressing partial potentials for energy conservation at the sequential energy bifurcations from exciton to the reduction of intersystem electron acceptors and to the reduction of PS I end acceptors, respectively. At each energy bifurcation, the partial potential is given by the ratio of the efficiency for energy conservation divided by the complementary of this efficiency (the latter is given in brackets for each white arrow in Fig. 1). The RC/ABS is also an expression of partial potential denoted by γ_{RC}. It is the fraction of PS II Chl *a* molecules that function as RCs ($\gamma_{RC} = Chl_{RC}/Chl_{total}$) and since $Chl_{total} = Chl_{antenna} + Chl_{RC}$, we obtain $\gamma_{RC}/(1 - \gamma_{RC}) = Chl_{RC}/Chl_{antenna} \propto RC/ABS$. The partial potentials are, therefore, given as: $\gamma_{RC}/(1 - \gamma_{RC})$ (or RC/ABS), $\varphi_{Po}/(1 - \varphi_{Po})$, $\psi_{Eo}/(1 - \psi_{Eo}]$ and $\delta_{Ro}/(1 - \delta_{Ro})$. We note that, according to their definition, both the PI_{ABS} and PI_{total} are indices of photosynthetic performance — on the basis of light absorption.

The performance index PI_{total} is the most sensitive parameter of the JIP-test because it incorporates several parameters that are evaluated from the fluorescence transient OJIP, e.g.,

- the maximum quantum yield of primary photochemistry, φ_{Po} (using F_0 and F_M)

- the probability to move an electron further than Q_A^-, ψ_{Eo} (using V_J)
- the probability to reduce an end electron acceptor, δ_{Ro} (using V_J and, in addition, V_I), and
- the RC/ABS ratio (using φ_{Po}, V_J and the initial slope of OJIP).

Therefore, any change in the OJIP transient is expressed in the PI_{total}, while the commonly used F_V/F_M is only sensitive to the ratio F_0/F_M.

3. Results and discussion

3.1. α- and γ-tocopherol levels and ratios

The effect of salt (NaCl), heavy metal (CdCl$_2$) and mannitol treatments on WT and TR (line 16.1) *B. juncea* plants is presented in Fig. 2. The upper panels (Fig. 2A, B and C) show α- and γ-tocopherol concentrations (pmol/mg fresh weight of 8 day old seedlings) in the WT plants (columns with grey and white areas) and in the TR (line 16.1) plants (columns with black and hatched areas). The lower panels (Fig. 2D, E and F) show the α-tocopherol/γ-tocopherol ratios in the WT (white dotted columns) and the TR (line 16.1) plants (grey dotted columns).

On administering NaCl to the WT *B. juncea* plants, the total tocopherol concentration (α-tocopherol plus γ-tocopherol) increased with increasing concentration of NaCl (2 fold at 100 mM and 2.3 fold at 200 mM NaCl). Although, the total tocopherol decreased with the further increase of NaCl (400 mM), it still remained higher (by 1.4 fold) than in the untreated control (without NaCl; control) plants (Fig. 2A). However, the decrease in total tocopherol at 400 mM NaCl

was solely due to the decrease of α-tocopherol (grey column-area), while the γ-tocopherol continued to increase (white column-area). This is clearly demonstrated by the α-tocopherol/γ-tocopherol ratio (Fig. 2D), which was higher at 100 mM (4.5) compared to the control (3.1), but decreased below the control (to 2.8) at 200 mM NaCl, dramatically dropping to 0.8 at 400 mM NaCl. This shows that there was a buildup of γ-tocopherol in the leaves in response to salt stress, which could not be efficiently converted to α-tocopherol presumably due to limitation of the activity of the γ-TMT enzyme. This is in agreement with the data on the WT and TR (line 16.1) plants treated with 400 mM NaCl. In the TR plants, the total tocopherol content (Fig. 2A) was only slightly higher (significant at $P = 0.08$, single tail) than in the WT plants. However, the α-tocopherol/γ-tocopherol ratio (Fig. 2D) was much higher in the TR plants (3) exposed to 400 mM NaCl as compared to the similarly treated WT plants (0.8). We conclude, based on these and other observations (see above) that overexpression of the γ-TMT gene retains the efficiency of γ-tocopherol to α-tocopherol conversion even under salt stress, without affecting the capability of the transgenic plants to increase the total tocopherol levels in response to stress.

The trend of the effect of CdCl$_2$ (Fig. 2B and E) was similar to that of NaCl treatment. However, the maximal increase of α-tocopherol (at 20–40 mM CdCl$_2$) was less extended (1.5 times the level in the control), while the γ-tocopherol increase was highly pronounced; at 40 mM CdCl$_2$, it was 9.3 fold higher than in the control. Further, the α-tocopherol/γ-tocopherol ratio decreased even at 10 mM CdCl$_2$ and dropped down, from 3.1 in the control, to 0.44 at 40 mM CdCl$_2$. As in the case of salt treatment (see above), overexpression of the γ-TMT
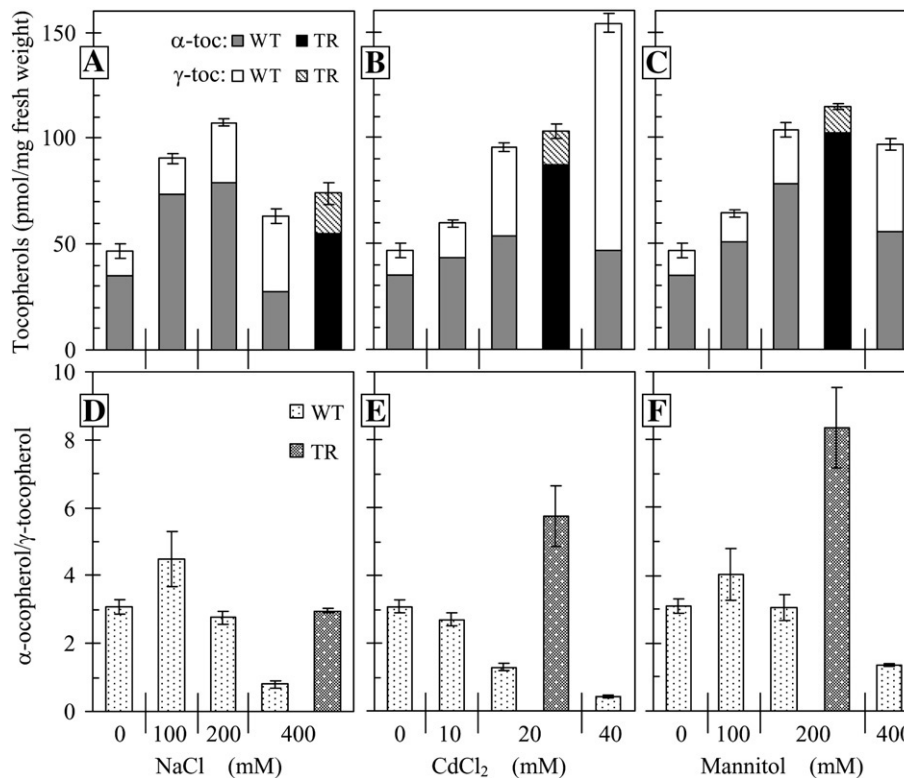

Fig. 2. Tocopherol levels and α-tocopherol/γ-tocopherol ratios in WT and TR (line 16.1) *B. juncea*, grown under different abiotic stress treatments. Concentration (pmol/mg fresh weight) of α-tocopherol and γ-tocopherol (upper panels; grey and white areas of the columns, respectively, as indicated in panel A) and α-tocopherol/γ-tocopherol ratios (lower panels; white dotted columns, as indicated in panel D) in the cotyledonary leaves of 8 day old seedlings of WT *B. juncea* treated with different concentrations of NaCl (panels A and D), CdCl$_2$ (panels B and E), and mannitol (panels C and F). The upper panels also depict the α- and γ-tocopherol concentration (black and hatched parts of the columns, respectively; as indicated in panel A) and the lower panels the α-tocopherol/γ-tocopherol ratio (grey dotted columns; as indicated in panel D) in the cotyledonary leaves of 8 day old seedlings of TR (line 16.1) *B. juncea* treated with 400 mM NaCl (panels A and D), 20 mM CdCl$_2$ (panels B and E) and 200 mM mannitol, (panels C and F). The values are means ± SE from three independent experiments (1 g of fresh cotyledonary leaves for each replicate); the error bars in the upper panels refer to the Standard Error (SE) of total tocopherol (= α-tocopherol + γ-tocopherol; total column height).

gene did not affect the total tocopherol content, but increased the α-tocopherol/γ-tocopherol ratio by 1.9 fold, which was even higher than in the untreated WT plants.

The impact of mannitol treatment on the WT plants (Fig. 2C and F) was very similar to that of the salt treatment. However, there seems to be a lower sensitivity of plants towards mannitol than towards NaCl, since (i) at 100 mM, the increase of tocopherol level was less under mannitol than under NaCl treatment and (ii) the increase of mannitol from 200 to 400 mM did not affect the tocopherol level unlike that with NaCl treatment. The comparison of the responses of transgenic (line 16.1) and wild type to mannitol treatment reveals that the α-tocopherol/γ-tocopherol ratio in the treated transgenic was higher than in the untreated wild type (by 2.7 fold).

In summary, results obtained with all the three treatments (salt, heavy metal, and mannitol), with both WT and TR (line 16.1) plants, show that overexpression of the γ-TMT gene did not affect the total tocopherol content but increased the efficiency of γ-tocopherol to α-tocopherol conversion. These results are in agreement with previous studies on tocopherol levels in other plants subjected to abiotic stress including high light, drought, salt, and cold (see Introduction). Collakova and DellaPenna [4] have reported an increase in the total tocopherol in A. thaliana leaves under stress, and accumulation of γ-tocopherol, as well as, enhanced γ-tocopherol to α-tocopherol conversion in the transgenic A. thaliana plants overexpressing the γ-TMT gene. Our results with the economically important B. juncea plants are consistent with those on the model organism A. thaliana.

3.2. Seed germination, shoot growth and leaf disc senescence under abiotic stress

Tocopherols are among the most powerful antioxidants present in the cell and are known to play an important role under stress conditions in concert with other antioxidants present in the cell (see Introduction). As we showed that TR (line 16.1) plants of B. juncea, overexpressing the γ-TMT gene, had higher α-tocopherol content than the WT plants (Fig. 2), we used them to test if the increased α-tocopherol content would confer advantage to the plants in tolerating abiotic stress. Thus, the tolerance of B. juncea plants to various abiotic stress treatments was assessed with measurements of seed germination, shoot growth and leaf disc senescence. We observed (Fig. 3) that the percentage germination of TR seeds on MS medium supplemented with 200 mM NaCl, 20 mM CdCl$_2$ and 200 mM mannitol was much higher (26.9%, 35.2% and 86.6%, respectively) than the germination of WT seeds under the same treatments (8.3%, 5.9% and 38%, respectively).
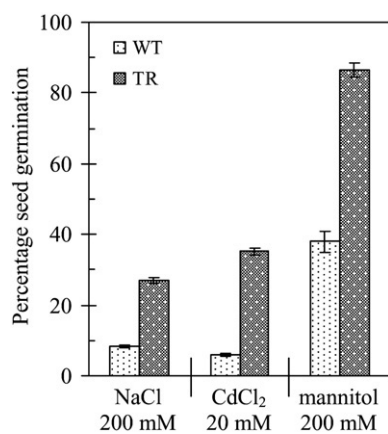

Fig. 3. Germination of WT and TR (line 16.1) B. juncea seeds under abiotic stress. Percentage germination of seeds from WT (dotted white columns) and TR (line 16.1) (dotted grey columns) B. juncea plants grown on MS medium supplemented with 200 mM NaCl, 20 mM CdCl$_2$ or 200 mM mannitol. The values are means ± SE from three independent experiments (50–60 seeds for each replicate).

In order to study the effects of the abiotic stress on shoot growth, seeds from TR B. juncea (line 16.1 and two additional lines 14.1 and 25.1) and WT plants were first germinated on MS medium. On day 5, the shoots were cut from beneath the cotyledonary leaves and placed on the same medium supplemented with 400 mM NaCl, 40 mM CdCl$_2$, and 200 mM mannitol. The shoots of the TR plants of B. juncea kept on NaCl supplemented medium appeared healthy and showed better growth than those of the WT plant, even after 15 days of stress (Fig. 4A). In CdCl$_2$ and mannitol treated plants, shoots of the WT almost bleached and died within 15 days while those from the TR plants were green and healthy (Fig. 4B and C). Among the three TR lines, line 16.1, which was the one with highest overexpression of the γ-TMT gene, was found to be most tolerant to the applied stresses.

The level of senescence of discs from young leaves of the TR (line 16.1) and WT B. juncea was assessed by their chlorophyll content. The content and distribution of tocopherol in young leaves (as used for leaf disc senescence assay and Chl a fluorescence measurements) was comparable to that measured in the small cotyledonary leaves. Furthermore, γ-TMT gene was overexpressed under the control of a strong constitutive (CaMV35S) promoter, and its expression in the young leaves was found to be high in northern blot experiments (data not shown). Fig. 5 shows the chlorophyll content (μg/g fresh weight) of leaf discs floated on MS medium supplemented with different concentrations of NaCl (Fig. 5A), CdCl$_2$ (Fig. 5B) and mannitol (Fig. 5C) for 7 days. Visual changes in leaf discs, under the corresponding treatment, are shown in the photographs (lower panels of Fig. 5). Both the upper and lower panels of Fig. 5 show that the decrease of Chl content was less in the treated TR (line 16.1) than in the WT plant, while both had the same Chl content when untreated. The Chl content in the TR plants was higher than in the WT by 1.4, 2.9 and 3.3 fold at 200, 400 and 800 mM NaCl, respectively (Fig. 5A), by 1.5, 3.3, and 4.0 fold at 10, 20, and 40 mM CdCl$_2$, respectively (Fig. 5B) and by 1.4, 2.7 and 3.6 fold at 100, 200, and 400 mM mannitol, respectively.

The above results show that, indeed, the TR (line 16.1) plants were more tolerant than the WT plants to the applied stress since the germination percentage (Fig. 3) and the shoot growth (Fig. 4) were significantly higher. Moreover, the leaf discs from the TR plants showed a delayed senescence as compared to the WT plant (Fig. 5).

Despite the known antioxidant roles of α-tocopherol in chloroplasts, studies by Porfirova et al. [28] and Kanwischer et al. [29] showed that in certain tocopherol-deficient mutant plants, α-tocopherol was not essential for plant survival under optimal conditions, and the growth and phenotype of the mutants was quite comparable to that of the wild type when exposed to various stresses. The reason for such an observation could be that α-tocopherol is one of the several members of the antioxidant network in the cells that include other components like ascorbate, glutathione, flavonoids and terpenoids [30]. Thus, loss of α-tocopherol could be compensated by the other compounds in maintaining the antioxidant status of the cells. In contrast, results obtained in the present study show that TR (line 16.1) plants having the same total tocopherol content as the WT plants were more tolerant to stress, which could only be related to their higher α-tocopherol level resulting from a more efficient conversion of γ- to α-tocopherol. This is in agreement with the different in vivo antioxidant activities of the two tocopherol forms against lipid oxidation, with one molecule of α-tocopherol protecting up to 220 and γ-tocopherol protecting up to 100 molecules of PUFA [3]. Further, increased α-tocopherol level was found to be essential for the tolerance of A. thaliana to Cu and Cd induced oxidative stress [8] and tocopherols have also been suggested to be involved in the adaptation of wheat plants to Ni induced stress [7].

Tocopherols have been shown to be present not only in thylakoid membranes but also in plastoglobules. Vidi et al. [31] have shown the localization of AtVTE1 encoding tocopherol cyclase in the plastoglobuli and the accumulation of about 36% of total chloroplast tocopherol in the plastoglobules of chloroplasts in Arabidopsis thaliana. However, they did
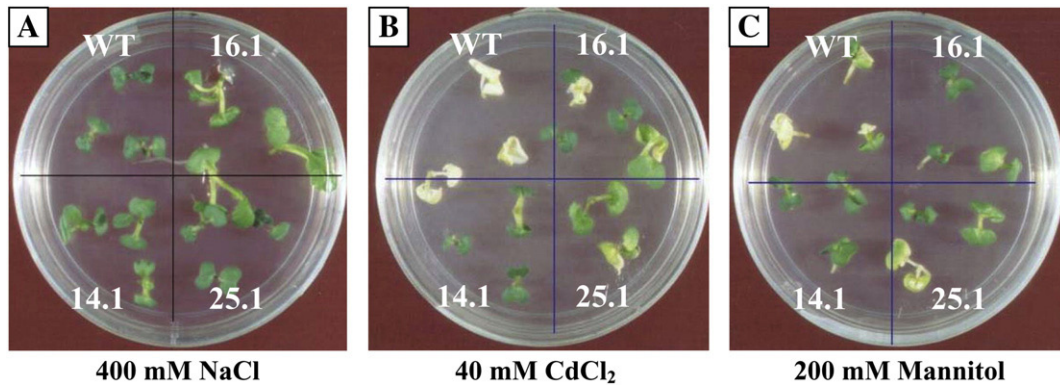
Fig. 4. Comparison of growth of shoots of WT and TR lines of *B. juncea* under abiotic stress. Shoots of WT and of three independent TR lines (14.1, 16.1 and 25.1, as indicated) of *B. juncea* grown on MS medium that was supplemented on day 5 with 400 mM NaCl (A), 40 mM CdCl₂ (B) and 200 mM mannitol (C); photographs were taken after 15 days.

not find the presence of other tocopherol biosynthesis enzymes (including γ-TMT enzyme, overexpressed in *Brassica juncea* in our study) in the plastoglobuli suggesting that the final methylation step does not take place in the plastoglobules. They postulated that plastoglobuli may be involved in trafficking of tocopherol biosynthetic intermediates and concluded that the "final destination of tocopherol is most likely the thylakoid membrane, where it has been shown to protect the Photosystem II and to prevent the oxidative degradation of fatty acids by scavenging reactive oxygen species". In an apparent contradiction, Matringe et al. [32] found the presence of tocopherols mostly in the thylakoid membranes of young tobacco leaves and a very miniscule (<1%) percentage of vitamin E, mostly δ-tocopherol, in the plastoglobuli. They, however, observed greater tocopherol levels in the plastoglobuli prepared from old and senescing leaves. These two studies point to the role that plastoglobules might be playing in storage and trafficking of tocopherols inside the chloroplasts. The presence of tocopherols in the plastoglobules in *Brassica* sp. has not been reported in the literature to the best of our knowledge. As the better photosynthetic performance of α-tocopherol enriched transgenic plants, under stress in our study, provides an indirect cue to the localization of tocopherols in the thylakoid membranes, we further evaluated the photosynthetic

performance, upto the reduction of PS I end electron acceptors of these plants by analyses of Chl *a* fluorescence measurements.

3.3. Analysis of OJIP fluorescence transients by the JIP-test — evaluation of photosynthetic performance

Chl *a* fluorescence transients of the dark-adapted leaves of *B. juncea* plants are shown, on logarithmic time scale from 10 μs up to 1 s, in Fig. 6A. Fluorescence transients of untreated WT plants and those treated with 200 mM NaCl, 20 mM CdCl₂ and 200 mM mannitol, are plotted with grey, light-blue, orange and light-green lines respectively; for the same treatment, fluorescence transients from the TR (line 16.1) plants are plotted with darker lines, i.e., black, blue, red and green. All curves show the typical OJIP shape (the O, J, I and P steps are marked in the plot), with similar maximum variable fluorescence $(F_M - F_0 = F_V)$, demonstrating that all samples were photosynthetically active. The differences among the eight cases are shown in Fig. 6B, where fluorescence data were normalized between the steps O (50 μs) and I (30 ms) and presented as relative variable fluorescence $W_{OI} = (F_t - F_0)/(F_I - F_0)$ vs. time (logarithmic time scale from 50 μs up to 1 s); we observe that the curves are grouped in
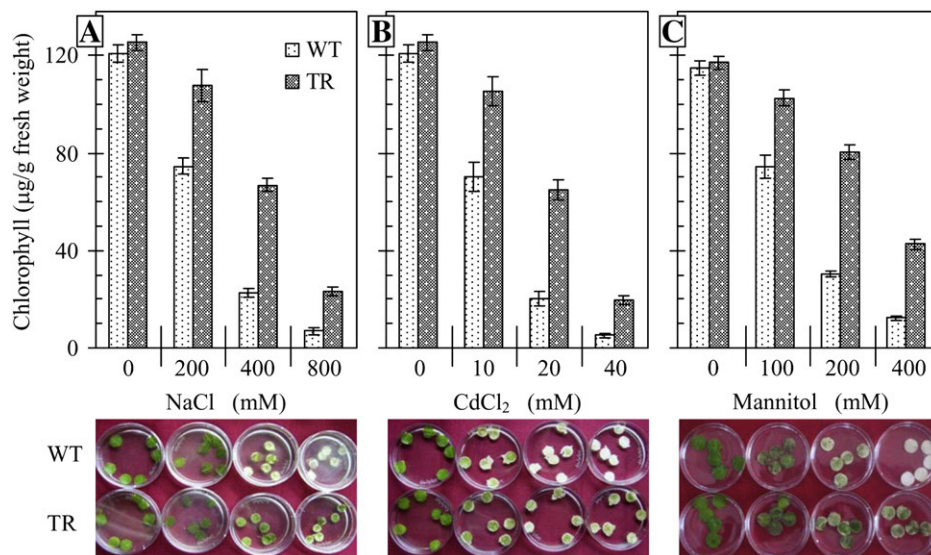

Fig. 5. Leaf disc senescence under abiotic stress as measured by chlorophyll content. Chlorophyll content (μg/g fresh weight) of leaf discs from WT (white dotted columns) and TR (line 16.1, grey dotted columns) untreated *B. juncea* plants, kept for 7 days at different concentrations (in distilled water) of NaCl (panel A), CdCl₂ (panel B) and mannitol (panel C); the values are means ± SE from three independent experiments (200 mg of the leaf discs for each replicate). Below each of the plots, photographs of the WT and TR leaf discs under the corresponding treatments are presented.
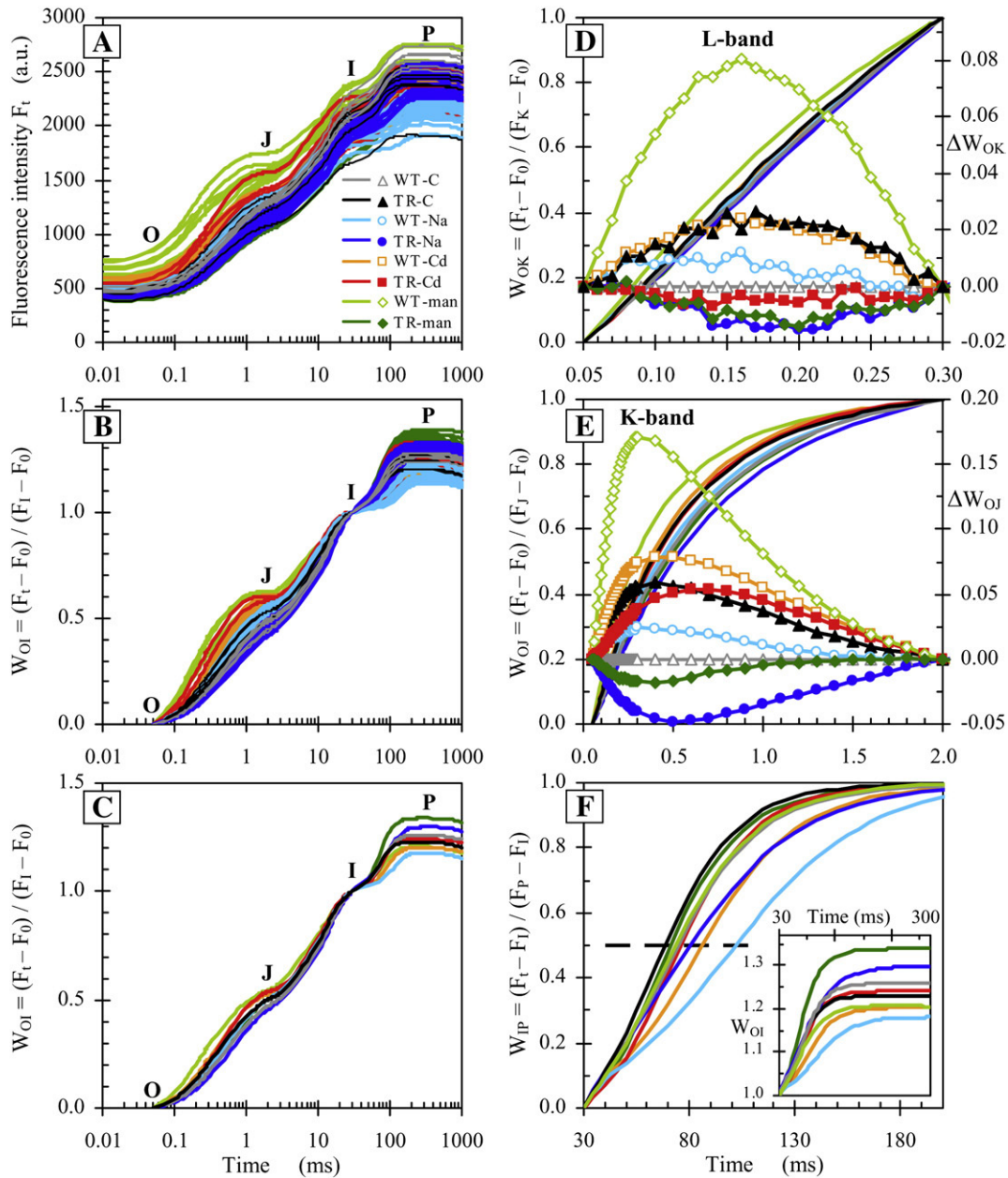
Fig. 6. Chl *a* fluorescence kinetics OJIP of dark adapted leaves of *B. juncea* plants, of all samples (panels A and B; 18 replicates) and average kinetics (panels C–F). Panel A: raw (direct) transients; panel B: $W_{OI} = (F_t - F_0)/(F_I - F_0)$; panel C: W_{OI} (A–C: on logarithmic time scale); panel D: $W_{OK} = (F_t - F_0)/(F_K - F_0)$; panel E: $W_{OJ} = (F_t - F_0)/(F_J - F_0)$; panel F: $W_{IP} = (F_t - F_I)/(F_P - F_I)$ and W_{OI} in the insert. In panels D and E, the difference kinetics $\Delta W = W - (W)_{WT-C}$, where "WT-C" stands for control (untreated) wild type, are also plotted (right vertical axis; open and closed symbols for WT and TR (line 16.1), respectively), revealing the L-band and K-band, respectively. As indicated (in panel A for the whole figure), grey, light-blue, orange and light-green colors (lines and symbols) refer to WT plants and correspond to untreated (C; triangles) and those treated with 200 mM NaCl (Na; circles), 20 mM CdCl$_2$ (Cd; squares) or 200 mM mannitol (man; diamonds), respectively; black, blue, red and green refer, accordingly, to TR (line 16.1) plants.

packages. This normalization serves to distinguish the sequence of events from exciton trapping by PS II up to plastoquinone (PQ) reduction (O–I phase; W_{OI} from 0 to 1), from the PS I-driven electron transfer to the end electron acceptors on the PS I acceptor side, starting at PQH$_2$ (plastoquinol) (I–P phases; $W_{OI} \geq 1$). The average W_{OI} kinetics are depicted in Fig. 6C.

To further evaluate the differences between various samples, we employed (see the other panels of Fig. 6), additional normalizations (left vertical axis) and corresponding subtractions (difference kinetics; right vertical axis). For this purpose, we used linear time scales. (*Note*: For all the plots of Fig. 6, lines refer to kinetics and lines with symbols to difference kinetics). The difference kinetics reveal

bands that are hidden between the steps O, J, I and P of the direct or normalized transients (see Materials and methods). As indicated in Fig. 6A, and for all plots, open and closed symbols refer to the WT and TR (line 16.1) plants, respectively. The symbols, with the same color code as for the lines, are: triangles for untreated/control (C) and circles, squares and diamonds for treatments with 200 mM NaCl (Na), 20 mM CdCl$_2$ (Cd) and 200 mM mannitol (man), respectively.

In Fig. 6D, the fluorescence data were normalized between the steps O (50 μs) and K (300 μs), as $W_{OK} = (F_t - F_0)/(F_K - F_0)$, and plotted with the difference kinetics $\Delta W_{OK} = W_{OK} - (W_{OK})_{WT-C}$ in the 50–300 μs time range. The L-band (see e.g. [33]) revealed by such a subtraction (at about 150 μs) is an indicator of the energetic

connectivity (grouping) of the PS II units, being higher when connectivity is lower [25]. Therefore, Fig. 6D demonstrates that, in the WT plant, all treatments resulted in a decrease of the energetic connectivity (positive L-bands), with the strongest effect exerted by mannitol treatment. We also show that the untreated TR plants had lower connectivity than the untreated WT plant (positive L-band), while the treated TR plants exhibited higher connectivity (negative L-bands) compared not only to the similarly treated WT but also to the untreated WT plants. A higher connectivity results in a better utilization of the excitation energy and a higher stability of the system [17,25].

In Fig. 6E, fluorescence data were normalized between the steps O and J (2 ms), as $W_{OJ} = (F_t - F_0)/(F_J - F_0)$, and plotted with the difference kinetics $\Delta W_{OJ} = W_{OJ} - (W_{OJ})_{WT-C}$ in the 50 μs–2 ms time range. The positive K-band (at about 300 μs) reflects either an inactivation of the oxygen evolving complex, and/or an increase of the functional PS II antenna size (see Materials and methods). Fig. 6E shows the same trend as in Fig. 6D, except for CdCl$_2$-treated TR plants, where the K-band is positive and has almost the same amplitude as the untreated TR plants (though shifted to about 700 μs).

To evaluate the I–P phase, two different normalization procedures were used (Fig. 6F). In the insert, fluorescence data were normalized between the steps O and I (i.e., W_{OI}), as in Fig. 6C, but here only the part with $W_{OI} \geq 1$ was plotted, in the 30–300 ms time range (linear scale). For each curve, the maximal amplitude of the fluorescence rise reflects the size of the pool of the end electron acceptors at the PS I acceptor side; the insert demonstrates that (a) in the WT plants, all treatments resulted in a decrease of this pool size, with the strongest effect caused by NaCl treatment, (b) the untreated TR (line 16.1) plants had a smaller pool than the untreated WT, and (c) the treated TR plants had a bigger pool compared to the similarly treated WT plants. In the main plot (Fig. 6F), fluorescence data were normalized between the steps I (30 ms) and P (peak), as $W_{IP} = (F_t - F_I)/(F_P - F_I)$, and plotted in the 30–200 ms range. This normalization, where the maximal amplitude of the rise was fixed at unity, facilitated a comparison of the reduction rates of the end electron acceptors' pool in various samples; their half-times are shown by the crossing of the curves with the horizontal dashed line drawn at $W_{IP} = 0.5$ (half rise). We observe that for each treatment, as well as for the untreated samples, the overall rate constant (inverse of the half-time) of the processes leading to the reduction of the end electron acceptors was higher in the TR than in the WT plants. We also observe that both in the WT and the TR plants, the treatments used resulted in a lower rate (bigger half-time), with the strongest effect caused by NaCl treatment. Comparison with the findings in the insert indicates that the regulation of the overall rate constant for the reduction of the end electron acceptor pool was independent of the regulation of the pool size.

The fluorescence transients depicted in Fig. 6A were also analyzed by the JIP-test to deduce 12 structural and functional parameters quantifying the photosynthetic behavior of the samples (see Materials and methods for the definition and derivation of the parameters). Fig. 7 shows the calculated average values of the photosynthetic parameters of the WT (open symbols; panel A) and the TR (line 16.1) plants (closed symbols; panel B) of *B. juncea*, that were either untreated (control; triangles) or treated with 200 mM NaCl (circles), 20 mM CdCl$_2$ (squares) or 200 mM mannitol (diamonds). [For the definition of the parameters, see Materials and methods]. For each parameter and for both the WT and the TR (line 16.1) plants, the values were normalized on that of the control (untreated) WT plants, which is presented in both the panels by a regular polygon (all parameters equal to unity; open triangles). Hence, the deviation of the behavior pattern in each case from the regular polygon demonstrates the fractional impact, compared to the untreated WT, of the corresponding treatment (including also the fractional difference of the untreated TR; closed triangles in panel B).

The sequence of parameters, referring to the sequential energy transduction, i.e., the energy fluxes for (light) *abs*orption (ABS), *tr*apping (TP$_0$), *e*lectron *t*ransport (ET$_0$) and *r*eduction of the *e*nd electron acceptors at the PS I acceptor side (RE$_0$), is indicated by the "energy cascade" arrow (Fig. 7). At the left of the arrow, the parameters are expressed per ABS and at the right, per RC (Reaction Center). The energy fluxes per RC are functional parameters (specific energy fluxes), while the energy fluxes per ABS express, by definition, the corresponding quantum yields, which are structural parameters. Here, the ratio RC/ABS is included in the energy cascade, as it is proportional to the fraction of absorbed energy by PS II antenna (excitation) that reaches the RCs.

The behavior patterns for the treated WT have similar shapes (Fig. 7), thus demonstrating that the three applied treatments affected the same components of the photosynthetic system, though to a different extent, with the strongest effect by mannitol treatment (as
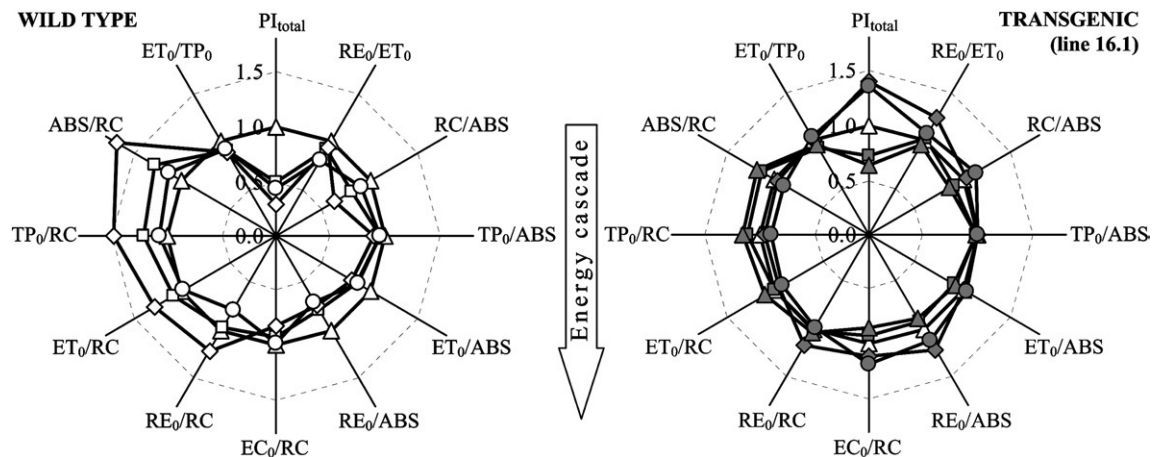

Fig. 7. Photosynthetic parameters deduced by the JIP test analysis of fluorescence transients (see Materials and methods). Behavior patterns of wild type (open symbols; left panel) and transgenic (line 16.1) (closed symbols; right panel) *B. juncea* plants, which were either untreated (control; triangles) or treated with 200 mM NaCl (circles), 20 mM CdCl$_2$ (squares) or 200 mM mannitol (diamonds) consist of 12 structural and functional photosynthetic parameters (average values of 18 replicates) derived by the JIP-test from the fluorescence transients shown in Fig. 6A. For each parameter and for both plant types the values were normalized, using as reference the control (untreated) wild type, presented in both panels by a regular polygon (all parameters equal to unity; open triangles). The deviation of the behavior pattern from the regular polygon demonstrates the fractional impact, compared to the untreated wild type, of the corresponding treatment (as well as the fractional difference of the untreated transgenic; closed triangles). The arrow indicates the sequence of events in the energy cascade (see Fig. 1), from absorption (ABS) up to the reduction of end electron acceptors at the PS I acceptor side, quantified by the fluxes per ABS (RC/ABS and quantum yields; at the left of the arrow) and per RC (specific fluxes; at the right of the arrow).

also revealed by the difference kinetics ΔW_{OK} and ΔW_{OJ} in Fig. 6). The various parameters were differentially affected: (a) the specific fluxes increased, except for the case of NaCl treatment where a decrease was observed; (b) the total electron carriers per reaction center, EC_0/RC, decreased in accordance with the data in the insert of Fig. 6F; (c) all the quantum yields decreased, with the effect on ET_0/ABS being larger than on TP_0/ABS and that on RE_0/ABS was still larger, since the efficiencies of the intermediate energy transduction, ET_0/TP_0 and RE_0/ET_0, also decreased (note that $ET_0/ABS = (TP_0/ABS).(ET_0/TP_0)$ and $RE_0/ABS = (ET_0/ABS).(RE_0/ET_0)$; see Materials and methods); (d) the RC/ABS decreased. The performance index PI_{total} (see Fig. 8) showed the largest difference (negative), since it expresses the overall potential for energy conservation that depends on all the efficiencies for the sequential energy transduction (see Materials and methods). Among all the other parameters, ABS/RC (or its inverse, RC/ABS) exhibited the largest change upon the applied treatments. Since all treatments resulted in ABS/RC increase, the specific fluxes, which are products of the corresponding quantum yields and ABS/RC, also increased.

An increase of ABS/RC, which is a measure of the apparent antenna size (total absorption or total Chl per active RC), may either mean that (i) a fraction of RCs is inactivated e.g., by being transformed to non-Q_A-reducing centers, or (ii) the functional antenna, i.e., the antenna that supplies excitation energy to active RCs, has increased in size. In the first case, the TP_0/RC could not be affected (since it refers only to the active RCs) and, thus, TP_0/ABS (which is due to the trapping of excitation energy by the active RCs per total absorption) would decrease proportionally to RC/ABS (inverse of ABS/RC). In the second case, TP_0/ABS would proportionally follow the ABS/RC and, thus, TP_0/ABS is not affected. We observe here that the ABS/RC increase was accompanied by an increase of TP_0/RC, which, however, had a slightly different value (note that TP_0/ABS decreases). This suggests that changes took place both in the fraction of RCs transformed to non-Q_A-reducing centers and in the functional antenna size. However, even if the increase in the size of functional antenna would be related to the

energy supply to the active RCs from antenna that are associated with inactive RCs, the observation that TP_0/RC did not follow the ABS/RC increase means that there were, still, absorbing antenna Chls that did not feed the active RCs but dissipated their excitation energy by heat. From our results, we can not conclude whether the transformation of RCs to non-Q_A-reducing centers was due to inactivation of the oxygen evolving complex and/or due to their structural transformation to heat sinks (denoted also as silent centers [17]) that dissipated their excitation energy, as heat, instead of utilizing it to reduce Q_A.

In brief, the behavior patterns of the WT plants showed a "loss" in the ability for energy conservation after they were subjected to salt (NaCl), heavy metal ($CdCl_2$) or osmotic (mannitol) stress. This conclusion is in agreement with results obtained by normalization/subtraction of the fluorescence transients (see earlier discussion). However, the behavior patterns provided further quantitative information. The behavior pattern of the untreated TR (line 16.1) plants resembled that of the stressed WT plants (Fig. 7A), i.e., it exhibited a "loss" of the ability for energy conservation. Upon $CdCl_2$ treatment, the "loss" became smaller. However, upon NaCl or mannitol treatment, the patterns in the TR (line 16) plants, revealed a "gain" in the ability for energy conservation, when compared to the untreated WT plants.

The performance index PI_{total} of dark-adapted intact leaves, which includes partial "potentials" for energy conservation, is closely related to the final outcome of plant's activity, such as growth or survival under stress conditions (see e.g. [18,20,21]). PI_{total} is the most sensitive parameter of the JIP-test, as explained under Materials and methods. Note that a negative value of PI_{total} expresses a "loss" and a positive one expresses a "gain" in the ability for energy conservation. We present the PI_{total} for all the samples to facilitate a comparison among them. The average values of PI_{total}, calculated with the JIP-test from the direct fluorescence transients of untreated (triangles) and treated with 200 mM NaCl (+Na; circles), 20 mM $CdCl_2$ (+Cd; squares) or 200 mM mannitol (+man; diamonds) wild type (grey symbols) and transgenic (black symbols) plants, are presented without normalization, so that they can be compared with measurements in other investigations (Fig. 8). Thin hatched arrows indicate the change of PI_{total} caused by three treatments (salt, heavy metal, and mannitol), as compared to the corresponding untreated (control) case (the grey-hatching is for the WT and the black-hatching is for the TR (line 16.1) plants). Wide white arrows show the difference between the TR and the WT plants for each treatment.

Figure 8 shows that for the untreated plants, the PI_{total} of the transgenics was lower than that of the wild type plants. However, under each of the applied treatments, the PI_{total} of the wild type dropped extensively (downwards grey-hatched arrows) showing loss, which means there was a negative "strain" on the system, while in the transgenic plants the PI_{total} exhibited a wide increase (upwards black-hatched arrows) showing gain, which means that there was a positive "strain" on the system after NaCl and mannitol treatments, while a smaller (non significant) increase was observed after $CdCl_2$ treatment (compared to the untreated TR plant). Moreover, the negative "strain" observed in the WT plant under NaCl or mannitol stress was not only alleviated (white wide arrows), but the PI_{total} was even higher than that of the untreated WT plant; this does not hold true for $CdCl_2$ stress, though PI_{total} of the TR plant was again higher than that of the WT plant under the same stress. Fig. 8 clearly demonstrates that the structural modifications induced in the TR (line 16.1) plants enabled the photosynthetic machinery of those plants to perform better under salt, heavy metal and osmotic stress conditions.

The PI_{total} is an index of photosynthetic performance on the basis of light absorption (see Materials and methods). It does not necessarily reflect the performance of the whole plant that is governed by much more complex mechanisms. However, in several studies on stress a strong correlation was found between PI_{total} and physiological parameters, such as plant growth or survival rate
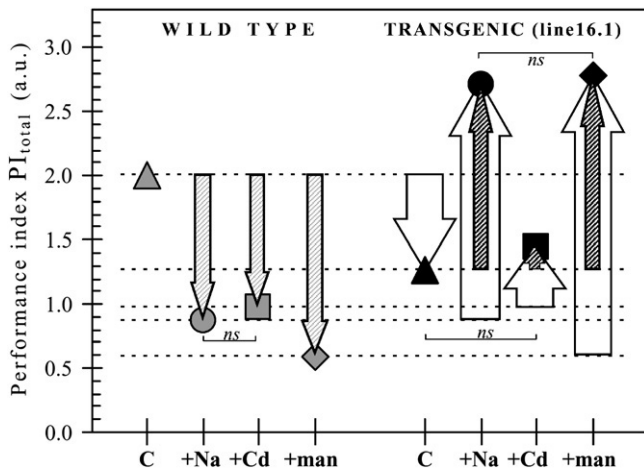

Fig. 8. Comparison of the performance index of the wild type and transgenic (line 16.1) *B. juncea* plants grown with or without abiotic stress. The performance index PI_{total} (in arbitrary unit, a.u.) was derived by the JIP-test from chlorophyll fluorescence transients (shown in Fig. 6A) of dark-adapted intact leaves from wild type (grey symbols) and transgenic (line 16.1, black symbols) *B. juncea* plants that were either untreated (C; triangles), or treated with 200 mM NaCl (+Na; circles), 20 mM $CdCl_2$ (+Cd; squares) or 200 mM mannitol (+man; diamonds). The values are means of 18 replicates; all the differences except those marked as "ns" (not significant) are statistically significant ($P<0.025$; one tail). Thin hatched arrows indicate the change of PI_{total} caused by the abiotic stress treatments, as compared to the corresponding untreated (control) case; grey-hatching is for wild type (downwards arrows — loss) and black-hatching is for the transgenic (line 16.1) plants (upwards arrows — gain). Wide white arrows show, for each treatment, the difference between transgenic (line 16.1) and wild type plants; there is a loss in the untreated and gain (alleviation of stress effect) in the treated plants.

[20,21]. This was not the case in the present study. One month after the fluorescence measurements (data not shown), the height of the plants was about the same in the treated and untreated plants, although the TR (line 16.1) plants were bigger by about 25%. On the other hand, crop yield (seed weight per plant) of the treated plants was lower than in the untreated plants, with the lowering being much more pronounced in the WT plants (by about 52% after NaCl, 66% after $CdCl_2$ and 60% after mannitol treatment) than in the TR (line 16.1) plants (by about 23% 37% and 42%, respectively).

Several non-antioxidant functions of tocopherols have been suggested in plants (as in animals) including their role in membrane stability and fluidity. α-tocopherol has been shown to play a role in vesicle stability and lipid dynamics using liposomes mimicking plant chloroplast membranes [34]. It is possible that the better performance of the transgenics in our present study might, in part, be due to such non-antioxidant functions of tocopherols. However, in this investigation we focused on the effects of increased α-tocopherol content on various components of the photosynthetic machinery as revealed by chlorophyll *a* fluorescence measurements. The other interactions warrant further investigations which form part of future studies.

4. Conclusion

Our results implicate the role of enhanced α-tocopherol, the most potent form of tocopherol, in the alleviation of stress induced by salt, heavy metal and mannitol in transgenic *B. juncea*. In the transgenic plants (line 16.1) overexpressing the γ-TMT gene, the increased conversion of γ-tocopherol to α-tocopherol was found to be associated with enhanced tolerance of the plants to various stresses. This was reflected in the photosynthetic performance, up to the reduction of PS I end electron acceptors and in several physiological parameters, i.e., seed germination, shoot growth and leaf disc senescence. The finding that the photosynthetic performance on the basis of light absorption was even better, in transgenic plants growing under different abiotic stress conditions than in the unstressed wild type plants indicates an up-regulation of the efficiency of the photosynthetic machinery related to the higher α-tocopherol content in the transgenic vs. the unstressed wild type plant. Further investigations are needed to resolve the relation between mechanisms regulating stress alleviation at different levels of plant performance.

Acknowledgements

References

[1] C. Schneider, Chemistry and biology of vitamin E, Mol. Nutr. Food Res. 49 (2005) 7–30.
[2] M.J. Fryer, The antioxidant effects of thylakoid vitamin E (α-tocopherol), Plant Cell Environ. 15 (1992) 381–392.
[3] K. Fukuzawa, A. Tokumura, S. Ouchi, H. Tsukatani, Antioxidant activities of tocopherols on Fe^{2+}-ascorbate induced lipid peroxidation in lecithin liposomes, Lipid 17 (1982) 511–513.
[4] E. Collakova, D. DellaPenna, Homogentisate phytyltransferase activity is limiting for tocopherol biosynthesis in *Arabidopsis*, Plant Physiol. 131 (2003) 632–642.
[5] H. Maeda, W. Song, T.L. Sage, D. DellaPenna, Tocopherols play a crucial role in low-temperature adaptation and phloem loading in *Arabidopsis*, Plant Cell 18 (2006) 2710–2732.
[6] S. Munne-Bosch, L. Alegre, The function of tocopherols and tocotrienols in plants, Crit. Rev. Plant Sci. 21 (2002) 31–57.
[7] E. Gajewska, M. Skłodowska, Relations between tocopherol, chlorophyll and lipid peroxides contents in shoots of Ni-treated wheat, J. Plant Physiol. 164 (2007) 364–366.
[8] V.C. Collin, F. Eymery, B. Genty, P. Rey, M. Havaux, Vitamin E is essential for the tolerance of *Arabidopsis thaliana* to metal-induced oxidative stress, Plant Cell Environ. 31 (2008) 244–257.
[9] A. Melis, Photosystem II-damage and repair cycle in chloroplasts: what modulates the rate of photodamage in vivo? Trends Plant Sci. 4 (1999) 130–135.
[10] B. Halliwell, J.M.C. Gutteridge, Free Radicals in Biology and Medicine, Oxford University Press (Clarendon), New York, 1989.
[11] J. Kruk, H. Hollander-Czytko, W. Oettmeier, A. Trebst, Tocopherol as singlet oxygen scavenger in photosystem II, J. Plant Physiol. 162 (2005) 749–757.
[12] A. Krieger-Liszkay, A. Trebst, Tocopherol is the scavenger of singlet oxygen produced by the triplet states of chlorophyll *a* in the photosystem II reaction center, J. Exp. Bot. 57 (2006) 1677–1684.
[13] J. Kruk, K. Strzalka, Redox changes of cytochrome b_{559} in the presence of plastoquinones, J. Biol. Chem. 276 (2001) 86–91.
[14] A. Gilmore, Govindjee, How higher plants respond to excess light: energy dissipation in photosystem II, in: G.S. Singhal, G. Renger, K.D. Irrgang, Govindjee, S. Sopory (Eds.), Concepts in Photobiology: Photosynthesis and Photomorphogenesis, Narosa Publishers/Kluwer Academic Publishers, 1999, pp. 513–548.
[15] D. Demming-Adams, W.W. Adams, A.K. Mattoo (Eds.), Photoprotection, Photoinhibition, Gene regulation, and Environment, Advances in Photosynthesis and Respiration, vol. 21, 2004, reprinted in softcover in 2008.
[16] M.A. Yusuf, N.B. Sarin, Antioxidant vitamin E addition in human diets: genetic transformation of *Brassica juncea* with γ-TMT gene for increased α-tocopherol content, Transgenic Res. 16 (2007) 109–113.
[17] R.J. Strasser, A. Srivastava, M. Tsimilli-Michael, Analysis of fluorescence transient, in: G. Papageogiou, Govindjee (Eds.), Chlorophyll Fluorescence: a Signature of Photosynthesis, Advances in Photosynthesis and Respiration, vol. 19, Springer, Dordrecht, 2004, pp. 321–362.
[18] M. Tsimilli-Michael, R.J. Strasser, In vivo assessment of plants' vitality: applications in detecting and evaluating the impact of Mycorrhization on host plants, in: A. Varma (Ed.), Mycorrhiza: State of the Art, Genetics and Molecular Biology, Eco-Function, Biotechnology, Eco-Physiology, Structure and Systematics, 3rd edition, Springer, Dordrecht, 2008, pp. 679–703.
[19] R.J. Strasser, A. Srivastava, Govindjee, Polyphasic chlorophyll *a* fluorescence transient in plants and cyanobacteria, Photochem. Photobiol. 61 (1995) 32–42.
[20] R.J. Strasser, M. Tsimilli-Michael, D. Dangre, M. Rai, Biophysical phenomics reveals functional building blocks of plants systems biology: a case study for the evaluation of the impact of Mycorrhization with *Piriformospora indica*, in: A. Varma, R. Oelmüler (Eds.), Advanced Techniques in Soil Microbiology, Soil Biology, 2007, Berlin Heidelberg, 2007, pp. 319–341.
[21] S. Zubek, K. Turnau, M. Tsimilli-Michael, R.J. Strasser, Response of endangered plant species to inoculation with arbuscular mycorrhizal fungi and soil bacteria, Mycorrhiza 19 (2009) 113–123.
[22] T. Murashige, F. Skoog, A revised medium for rapid growth and bio-assay with tobacco tissue cultures, Physiol. Plant. 15 (1962) 473–497.
[23] D.I. Arnon, Copper enzymes in isolated chloroplasts: polyphenol oxidase in *Beta vulgaris*, Plant Physiol. 24 (1949) 1–15.
[24] G.C. Papageorgiou, Govindjee (Eds.), Chlorophyll Fluorescence: a Signature of Photosynthesis, Advances in Photosynthesis and Respiration, vol. 19, Springer, Dordrecht, 2004.
[25] R.J. Strasser, The grouping model of plant photosynthesis: heterogeneity of photosynthetic units in thylakoids, in: G. Akoyunoglou (Ed.), Photosynthesis: Proceedings of the Vth International Congress on Photosynthesis, Halkidiki-Greece 1980, vol. III, Structure and Molecular Organisation of the Photosynthetic Apparatus, Balaban International Science Services, Philadelphia, 1981, pp. 727–737.
[26] G. Paillotin, Movement of excitations in the photosynthetic domains of photosystem I, J. Theor. Biol. 58 (1976) 337–352.
[27] B. Genty, J.M. Briantais, N.R. Baker, The relationship between the quantum yield of photosynthetic electron transport and quenching of chlorophyll fluorescence, Biochim. Biophys. Acta 990 (1989) 87–92.
[28] S. Porfirova, E. Bergmuller, S. Tropf, R. Lemke, P. Dormann, Isolation of an *Arabidopsis* mutant lacking vitamin E and identification of a cyclase essential for all tocopherol biosynthesis, Proc. Natl. Acad. Sci. USA 99 (2002) 12495–12500.
[29] M. Kanwischer, S. Porfirova, E. Bergmuller, P. Dormann, Alterations in tocopherol cyclase activity in transgenic and mutant plants of *Arabidopsis* affect tocopherol content, tocopherol composition, and oxidative stress, Plant Physiol. 137 (2005) 713–723.
[30] S. Munné-Bosch, The role of α-tocopherol in plant stress tolerance, J. Plant Physiol. 162 (2005) 743–748.
[31] P.A. Vidi, M. Kanwischer, S. Baginsky, J.R. Austin, G. Csucs, P. Dormann, F. Kessler, C. Brehelin, Tocopherol cyclase (VTE1) localization and vitamin E accumulation in chloroplast plastoglobule lipoprotein particles, J. Biol. Chem. 281 (2006) 11225–11234.
[32] M. Matringe, B. Ksas, P. Rey, M. Havaux, Tocotrienols, the unsaturated forms of vitamin E, can function as antioxidants and lipid protectors in tobacco leaves, Plant Physiol. 147 (2008) 764–778.
[33] A. Stirbet, Govindjee, B.J. Strasser, R.J. Strasser, Chlorophyll *a* fluorescence induction in higher plants: modelling and numerical simulation, J. Theor. Biol. 193 (1998) 131–151.
[34] D.K. Hincha, Effects of α-tocopherol (vitamin E) on the stability and lipid dynamics of model membranes mimicking the lipid composition of plant chloroplast membranes, FEBS Lett. 582 (2008) 3687–3692.